Published in final edited form as:
Nanomedicine (Lond). 2012 June ; 7(6): 815–833. doi:10.2217/nnm.11.156.

Blood-Borne Macrophage-Neural Cell Interactions Hitchhike Endosome Networks for Cell-Based Nanozyme Brain Delivery

Matthew J. Haney[1,2], **Poornima Suresh**[1,2], **Yuling Zhao**[1,2], **Georgette D. Kanmogne**[3,4], **Irena Kadiu**[1,2], **Marina Sokolsky-Papkov**[1,2], **Natalia L. Klyachko**[5], **R. Lee Mosley**[1,3,4], **Alexander V. Kabanov**[1,2,5], **Howard E. Gendelman**[1,3,4], and **Elena V. Batrakova**[1,2,*]

[1]Center for Drug Delivery and Nanomedicine, University of Nebraska Medical Center, Omaha, Nebraska, USA

[2]Department of Pharmaceutical Sciences, University of Nebraska Medical Center, Omaha, Nebraska, USA

[3]Center for Neurodegenerative Disorders, University of Nebraska Medical Center, Omaha, Nebraska, USA

[4]Department of Pharmacology and Experimental Neuroscience, University of Nebraska Medical Center, Omaha, Nebraska, USA

[5]Deparment of Chemical Enzymology, Faculty of Chemistry, M.V. Lomonosov Moscow State University, Moscow, Russia

Abstract

Background—Macrophage carried nanoformulated catalase ("nanozyme") attenuates neuroinflammation and protects nigrostriatal neurons from 1-methyl-4-phenyl-1,2,3,6-tetrahydropyridine intoxication. This is facilitated by effective enzyme transfer from blood borne macrophages to adjacent endothelial cells and neurons leading to the decomposition of reactive oxygen species.

Methods—We now examine the intra- and intercellular trafficking mechanisms of nanozymes.

Results—In macrophages, nanozymes are internalized mainly by clathrin mediated endocytosis then traffic to recycling endosomes. The enzyme is subsequently released in exosomes facilitated by bridging conduits. Nanozyme transfer from macrophages to adjacent cells by endocytosis-independent mechanisms diffusing broadly throughout the recipient cells. In contrast, macrophage-free nanozymes are localized in lysosomes following endocytic entry.

Conclusion—Facilitated transfer of nanozyme from cell to cell can improve neuroprotection against oxidative stress commonly seen during neurodegenerative disease processes.

Keywords

blood-brain barrier; cell-mediated drug delivery; catalase; exosome; intracellular localization; macrophage; nanozyme; Parkinson's disease

*Correspondence: Elena V. Batrakova, Center for Drug Delivery and Nanomedicine, 985830 Nebraska Medical Center, Omaha, NE 68198-5830; Tel: (402) 559-9364 ; Fax (402) 559-9365, ebatrako@unmc.edu.

INTRODUCTION

The pathobiology of neurodegenerative disorders, including Parkinson's and Alzheimer's diseases (PD and AD), is linked to microglial activation and its secretion of neurotoxic factors. These include reactive oxygen and nitrogen species (ROS and RNS) leading to oxidative stress and neuronal injuries [1–4]. Oxidative stress affects neuronal, astrocyte, and microglia function by inducing ion transport, calcium mobilization, and activating apoptotic programs. Apoptosis and excitotoxicity are principal causes of mitochondrial-induced neuronal death [5]. Indeed, the mitochondrial respiratory chain affects oxidative phosphorylation and is responsible for ROS production. Such pathways lead to neuronal demise and underlie the pathobiology of PD and AD [6]. The lack of natural antioxidants (glutathione and superoxide dismutase) and iron in the *substantia nigra* are specifically associated with the pathobiology of PD [7–9]. Thus, removing ROS and affecting mitochondria function through targeted delivery of redox enzymes could attenuate disease progression [10]. On balance, antioxidants when administered as therapeutic agents fail to alter the course of PD-associated neurodegeneration [11]. We posit that such failures may limit the delivery of antioxidants at disease sites. To this end, we developed a cell-based delivery system to bring nanoformulated catalase to affected brain regions in the 1-methyl-4-phenyl-1,2,3,6-tetrahydropyridine model (MPTP) of PD [12, 13]. The system rests in the abilities of blood borne macrophages to carry antioxidant proteins across the blood-brain barrier (BBB) to affected brain subregions. To preclude macrophage-mediated enzyme degradation, catalase was packaged into a block ionomer complex with a cationic block copolymer, poly(ethyleneimine)-poly(ethylene glycol). First, we reported that both components of the formulation, nanozyme and macrophages, were detected in the brain area of the MPTP-intoxicated animals [14]. Next, the formulation demonstrated efficient protection of enzymatic activity along with relatively high loading and release rates from bone marrow-derived macrophages (BMM) and limited cytotoxicities [14].

We propose that several independent processes serve to improve nanozyme-loaded macrophage therapeutics [15]. *First*, drug-loaded macrophages reach CNS inflammation sites and release catalase, and as such permit targeted therapeutic tissue-specific delivery [13]. *Second*, nanozyme-loaded macrophages permit sustained release of catalase allowing enzyme to enter the brain, independent of carrier cells. *Third*, catalase released from immunocytes such as macrophages can suppress peripheral leukocyte activation and protect nigrostratial neurons at a distance. *Fourth,* drug-loaded BMM transfer catalase nanoparticles to brain microvessel endothelial cells, neurons and astrocytes [15] and increase BBB penetration and ROS decomposition. Such events occur through endocytosis-independent mechanisms including fusion of cellular membranes, macrophage bridging conduits engagements of neighboring cells, and nanozyme lipid coating facilitating nanozyme transfer from carrier cells to target recipient cells [15]. Taken together, cell-to-cell transfer of nanozyme improves therapeutic outcomes afforded by catalase in PD mouse models. In the present study we uncovered the mechanisms for nanozyme trafficking in BMM and its transfer to endothelial cells and neurons. Nanozyme trafficking in and between cells can facilitate neuroprotective responses and provide insights into how cell-carried nanoformulations can inevitably improve clinical outcomes for neurodegenerative diseases.

MATERIALS & METHODS

Reagents

Catalase from bovine liver erythrocytes was provided by Calbiochem (San Diego, CA). Methoxypolyethylene glycol epoxy (Me-PEG-epoxy) was purchased from Shearwater Polymer Inc. (Huntsville, AL). Polyethyleneimine-poly(ethylene glycol) (PEI (2K)-PEG (10K)) was synthesized as described [12] by conjugation of PEI and Me-PEG-epoxy.

LysoTracker Green, MitoTracker Green, and ERTracker Green were obtained from Molecular Probes (Carlsbad, CA). Lipopolysaccharides (LPS), Sephadex G-25, Triton X-100, and trypsin were purchased from Sigma-Aldrich (St. Louis, MO). Cell dyes 1,1'-dioctadecyl-3,3,3',3'-tetramethylindodicarbocyanine perchlorate (DiD) and 3,3'-dilinoleyl-oxacarbocyanine perchlorate (DiO) were purchased from Invitrogen. FITC-conjugated mouse antibodies to EEA1 (early endosomes), and LAMP1 (lysosomes); and unconjugated mouse antibodies to Rab11 (recycling endosomes), and Alexa Fluor-405-conjugated anti-CD14 were purchased from BD Biosciences (San Diego, CA). Mouse monoclonal antibodies to RAB 7 (late endosomes) were obtained at Abcam (Cambridge, MA). Secondary goat antimouse FITC-conjugated antibodies were purchased from Invitrogen Interferon gamma (INF-γ) was purchased from Peprotech Inc. (RockyHill, NJ).

Catalase Nanozyme

The polycomplex was produced by mixing catalase and a block copolymer, PEI-PEG, which form nanoparticles with an enzyme-polyion complex core and PEG corona [12, 13] at charge ratio (Z = 1). This was calculated by dividing the amount of amino groups in the block copolymer protonated at pH 7.4 [16] by the total amount of Gln and Asp in catalase. For confocal studies, catalase was labeled with Alexa Fluor 647 Protein Labeling Kit (Invitrogen), or rhodamine isothiocyanate (RITC) [12]. Labeled catalase was purified from low molecular weight residuals by gel filtration on a Sephadex G-25 column, and lyophilized.

Cells

Bone marrow-derived macrophages (murine macrophages) were extracted from femurs of C57Bl/6 male mice 6–7 weeks of age according to previously published protocols [17] and cultured for 12 days in DMEM medium (Invitrogen) supplemented with 1,000 U/mL macrophage colony-stimulating factor (MCSF), a generous gift from Pfizer Pharmaceuticals, Cambridge, MA). Murine macrophages were collected after 12 – 14 days of culture. Human monocyte-derived macrophages were obtained from leukopaks of healthy donors, purified by countercurrent centrifugal elutriation [18] and cultured with MCSF.

Mouse catecholaminergic CATH.a neurons were purchased from American Type Culture Collection (ATCC, Manassas, VA, USA), and cultured in RPMI-1640 medium supplemented with 8% normal horse serum (NHS), 4% fetal bovine serum (FBS), and 1% penicillin-streptomycin. Cultures were maintained in a humidified incubator at 37°C and 5% CO_2. CATH.a neurons were differentiated by adding 1 mM of N6,2'-O-dibutyryladenosine 3',5'-cyclic monophosphate sodium salt (dbcAMP, Sigma-Aldrich) to the culture media every other day for 6–8 days.

Primary human brain microvessel endothelial cells (HBMEC) were isolated from brain tissue obtained during surgical removal of epileptogenic cerebral cortex in adult patients, and were provided by Drs Marlys Witte and Michael Bernas (University of Arizona, Tucson, AZ). Routine evaluation for expression of von Willebrand factor (VWF), Ulex europeus lectin, and CD31 demonstrated that HBMECs were more than 99% pure. HBMECs were seeded in the collagen I-coated chamber of slides (500,000 cells/well), or 6-well tissue culture plates, and cultured to confluence in Microvascular Endothelial Cell Growth Medium-2 (EGM-2) BulletKit media (Cambrex, Walkersville, MD) supplemented with 5% fetal bovine serum (FBS). Only cells at passage 1 to 4 were used in this study.

Confocal Microscopy

Human or mouse bone marrow-derived macrophages grown in chamber slides (500,000 cells/well) [19] were exposed to Alexa Fluor 647-labeled nanozyme (50 μg/ml, Z=1) for

different time points (5 min, 15 min, 30 min, 60 min) at 37°C. For *entrance pathway* evaluation, living cells were stained with FITC-labeled transferrin (Tf, clathrin-mediated endocytosis, 25 μg/ml, 15 min), or cholera toxin B (CTB, caveolin-mediated endocytosis, 25 μg/ml, 15 min); or fixed with 4% PFA in 0.03 M sucrose for 20 min, and permeabilized with 0.2% saponin in 0.03 M sucrose for 5 min cells were stained with FITC-conjugated mouse anti-clathrin heavy chain antibodies (BD Transduction Laboratories), or Cy3 labeled anti-caveolin-1 antibodies (Sigma-Aldrich) according to manufacturer's protocol. For *intracellular trafficking* studies, cells were stained with antibodies to early, late, or recycling endosomes, and lysosomes. For this purpose, loaded with nanozyme cells were rinsed three times with 1% BSA in PBS, fixed and permeabilized. Following permeabilization, cells were incubated with FITC-conjugated EEA1 or LAMP 1 monoclonal antibodies (5 μg/ml, 1 hour, BD Transduction Laboratories), or unconjugated primary mouse monoclonal antibodies, Rab7 or Rab11 (5 μg/ml, 30 min, BD Transduction Laboratories). Cells treated with unconjugated primary mouse antibody were stained with FITC-conjugated secondary goat anti-mouse immunoglobulin G (5 μg/ml, 1 hour, Sigma-Aldrich). To distinguish between the carrier cells and target cells, human macrophages were labeled with Alexa Fluor-405-conjugated anti-CD14. For *release mechanism* evaluation, macrophages were co-stained with Alexa Fluor-488 mouse anti-β-tubulin (clone 5H1) or Alexa Fluor-488-phalloidin (BD Biosciences) for tubulin and actin visualization, respectively. Labeled cells were examined by a confocal fluorescence microscopic system ACAS-570 (Meridian Instruments, Okimos, MI) with argon ion laser and corresponding filter set. Digital images were obtained using the CCD camera (Photometrics) and Adobe Photoshop software. Quantification of immunostaining was performed with ImageJ software, utilizing JACoP plugins [20] to calculate Pearson's colocalization coefficients [21]. Comparison was performed on 7–10 sets of images acquired with the same optical settings.

Nanozyme Macrophages Loading and Release

To evaluate the involvement of different types of endocytosis, murine macrophages grown in 24-well plates (2.5×10^6 cells/plate) [19, 22] were pre-incubated with serum free, phenol red free DMEM, containing inhibitors of clatrin-mediated endocytosis, sucrose (0.25 M, 20 min) or dansylcaverdine (0.2 mM, 10 min); inhibitors of caveolea-mediated endocytosis, fillipin (1 μg/ml, 20 min) or nystatin (50 μg/ml15 min); an inhibitor of phagocytosis, cytochalasin b (10 μg/ml, 2 hours); an inhibitor of scavenger receptor, polyinosinis acid (10 μg/ml, 30 min); an inhibitor of pinocytosis, colchicine (100 μg/ml, 2 hours); or an inhibitor of macropinocytosis, rotterin (2 μM, 30 min). Following pre-incubation, the cells were treated with RITC-labeled nanozyme (0.5 mg/ml) in the presence of the corresponding inhibitor or assay buffer for one hour, washed, lysed with 1% Triton X100, and levels of fluorescence in each sample were measured by Shimadzu RF5000 fluorescent spectrophotometer. For release studies, murine macrophages loaded with nanozyme for one hour were incubated with fresh assay buffer for another hour; then the media was collected and the levels of released nanozyme were detected by fluorospectrophotometry. To evaluate the effect of activation on nanozyme release and intracellular distribution, murine macrophages were pre-incubated with 500 ng/ml LPS and 200 ng/ml IFN-γ for 24 hours. Amount of accumulated nanozyme was normalized for protein content and expressed in μg of enzyme per mg of the protein as means ± SEM (n = 4).

Isolation of Nanozyme Released in Exosomes from Macrophages

Murine macrophages were preloaded with fluorescently-labeled nanozyme for 1 hour (0.5 mg/ml protein, Z=1), washed three times with PBS, and fresh media was added to the cells. Media was collected after 2 hours, and exosomes with encapsulated nanozyme were purified using Exoquick Exosome Precipitation Solution (System Biosciences, Mountain View, CA).

Isolated exosomal fraction was added to CATH.a neurons and dynamics of nanozyme accumulation in target cells were visualized by confocal microscopy.

Transmission Electron Microscopy (TEM)

A drop of isolated exosomal fraction with incorporated nanozyme in PBS was placed on Formvar®-coated copper grid (150 mesh, Ted Pella Inc., Redding, CA). The dried grid containing exosomes were stained with vanadyl sulfate and visualized using a Philips 201 transmission electron microscope (Philips/FEI Inc., Briarcliff Manor, NY).

Murine macrophages were pre-loaded with gold nanoparticles for one hour, washed, and cocultured with CATH.a neurons for 18 hours. Following incubation, the cell samples were conventionally prepared, and visualized by FEI Quanta 200 SEM equipped with Bruker AXS Quantax XFlash 4010 x-ray microanalysis detector.

Fluorescence Activated Cell Sorting (FACS)

Amount of fluorescently labeled nanozyme accumulated in target cells was measured by FACS. Typically, monolayers of HBMEC seeded in 6-well plates (1×10^6 cells/well) were allowed to attach overnight, and then incubated for various time intervals with human macrophages (1×10^6 cells/well) loaded with catalase nanozyme or identical concentration of free nanozyme (without macrophages) as previously reported [15]. To evaluate involvement of chemichannels in nanozyme transfer, target CATH.a neurons were pre-incubated in PMA (300 nM) for one hour and then cocultured with murine macrophages preloaded with RITC-labeled nanozyme with or without PMA in the media for another two hours. Following incubation, cells were collected, and the amount of accumulated nanozyme in target cells was assessed by FACS. To distinguish between the carrier cells and target cells, human or murine macrophages were labeled prior to the addition to the receiver cells with Alexa Fluor-647-conjugated anti-CD14 or CD11b, respectively.

Neuronal Survival Studies

CATH.a neurons cultured in 6-well plates (1×10^6 cells/well) were incubated with 500 μM 6-hydroxydopamine (6-OHDA) and murine macrophages loaded with nanozyme, or the same concentration of free nanozyme (without carrier cells) for four hours. Prior to the addition, murine macrophages were incubated with catalase nanozyme (0.5 mg/ml, the highest non-toxic concentration of nanozyme) as previously reported [13]. At these levels, 1×10^6 macrophages resuspended in 1 ml of the media accumulated about 25 μg of nanozyme. Following incubation, all cells were collected, washed, stained with Alexa Fluor-488 LIVE/DEAD dye according to manufacturer's protocol, and the amount of LIVE/DEAD dye accumulated in the recipient cells was assessed by FACS. To distinguish between the carrier cells and target cells, murine macrophages were labeled with Alexa Fluor-678-conjugated anti-CD11b prior to the addition [15]. The neuronal survival was expressed as percentage of control CATH.a neurons that were incubated in neuronal complete media.

Gold Nanoparticles Preparation

Gold nanoparticles were prepared by mixing of 25 ml $HAuCl_4$ (0.5 mM) water solution with 25 ml Pluronic block copolymer F127 (10 mM) solution. The mixture was incubated at 55°C for 2 hours and the obtained nanoparticles were separated by centrifugal filtration at 1500 RPM using a filter with 100 kDa cutoff. Effective hydrodynamic diameter and zeta-potential of gold nanoparticles were measured by photon correlation spectroscopy using 'ZetaPlus' Zeta Potential Analyzer (Brookhaven Instruments, Santa Barbara, CA). The average diameter was 66.46± 0.52nm, the polydispersity index (PDI) value was 0.073± 0.004 nm and z-potential was −30.47± 1.76 nm.

Statistical Analysis

For the all experiments, data are presented as the mean ± SEM. Tests for significant differences between the groups were performed using a one-way ANOVA with multiple comparisons and *post-hoc* Fisher's pairwise comparisons using GraphPad Prism 5.0 (GraphPad software, San Diego, CA). A minimum p value of 0.05 was estimated as the significance level for all tests.

RESULTS

Mechanism of entry, intracellular trafficking, and release of nanozyme in i) cell carriers, macrophages, and ii) receiver cells, neurons and brain microvessel endothelial cells, were investigated.

I. Cell Carriers: Nanozyme Entry and Intracellular Trafficking in Macrophages

For optimal therapeutic efficacy of cell-based drug delivery, nanomaterials require specific intracellular entry and organelle localization. These are linked to particle size, shape, material composition, surface chemistry, and charge [23]. To these ends, we examined how nanozymes enter and traffic in macrophages through employing specific inhibitors and by colocalization of the nanozyme with specific intracellular compartments. Because murine neurons and human brain microvessel endothelial cells were further used as receiver cells, both murine bone marrow derived macrophages (BMM) and human monocyte derived macrophages (MDM) were examined in this study.

Internalization—Mononuclear phagocytes (MP; monocytes, macrophages, and dendritic cells) demonstrate robust phagocytic activity with engagement of the scavenger receptor [24]. Following internalization, phagosomes fuse with lysosomes, where cargos are efficiently degraded [24]. To assess this pathway, the effect of inhibitors of phagocytosis and its scavenger receptor (cytochalasin b and polyinosinic acid [25], respectively) on nanozyme accumulation in macrophages was evaluated. To ensure inhibition of phagocytosis, disruption of actin microfilaments in treated cells was visualized with Alexa Fluor-488-phalloidin (Figure S1). No significant effect on nanozyme uptake in BMM was found by phagocytosis and scavenger receptor inhibition (Figure 1A). This supports a phagocytosis-independent pathway of nanozyme entry, and linked likely to relatively small particle sizes and the stealth effects of the PEG corona.

It is well known that nanoparticles under 500 nm may enter the cells by clathrin-dependent and/or clathrin-independent endocytosis [23]. The latter processes include caveolae-mediated endocytosis, macropinocytosis, and caveolae-independent endocytosis. Noteworthy, a fraction of the vesicles within the cell matures into recycling endosomes, and is transported back to the plasma membrane [26]. To examine the role of these pathways for nanozyme entry, specific inhibitors of endocytosis were employed. Because most of inhibitors are not specific for the particular route of internalization, parallel experiments with a range of inhibitors was employed for the each type of endocytosis. Pretreatment with inhibitors of clathrin-mediated endocytosis, sucrose or dansylcaverdine, significantly (~50%) decreased accumulation of nanozyme in murine BMM, suggesting this process is regulated by clathrin-coated pits (Figure 1A). Blocking caveolae formation with fillipin or nystatin had lesser effect (~25% decrease) thus indicating less involvement of lipid rafts in nanozyme entry.

Confocal microscopy supported these results (Figure 1B and C, Table 1). Colocalization of nanozyme with transferrin (Tf), a marker of clathrin-coated pits [27], (20%–40% for all studied time points, Figure 1B, Table 1) demonstrated clathrin-mediated endocytosis of the

nanozyme. Colocalization with cholera toxin B (CTB), a caveolae marker [27], (1%–5%, Figure 1C, Table 1) suggested that a caveolae-dependent pathway of nanozyme entry was not a primary mechanism for entry. Similar results were obtained with antibody to clathrin and caveolae proteins in human MDM providing cross validation for the murine studies (Figure S2). Finally, inhibition of pinocytosis as well as macropinocytosis with colchicine and rottlerin, respectively, resulted in a 35%-32% decrease in nanozyme accumulation (Figure 1A). A major role of the clathrin-dependent pathway for the particles entry into macrophages suggested that considerable portion of internalized nanoformulated catalase may bypass lysosomal degradation, are sorted into recycling endosomes, and then released in active form.

Intracellular trafficking—Intracellular localization of nanozyme in human (Figure 2, and Table 1) and murine (Figure S3, and Table S1) macrophages were evaluated by staining intracytoplasmic organelles that included the acidified endosomes, endoplasmatic reticulum (ER), and mitochondria. Microphotographs demonstrated substantial colocalization of nanozyme with Lysotracker (50%–60%, Figures 2 A and S3 A, Tables 1 and S1), and to a lesser degree with ER- (10–18%, Figure 2 B and S3 B, Tables 1 and S1) and Mito-tracker (10–18%, Figure 2 C and S3 C, Tables 1 and S1). Interestingly, nanozyme was relocated to acidic endosomes from other cellular compartments at later time points (30–60 min, Table 1). Lysotracker staining allows the examination of nanoparticle intracellular localization in live cells [28]. However, the marker stains all acidic compartments including lysosomes, late endosomes and to some extent recycling endosomes. Therefore, to study nanozyme localization in greater detail, specific staining with antibodies to early, late, or recycling endosomes and lysosomes was performed in fixed human macrophages (Figure 3, Table 1). Nanozyme accumulated largely in recycling endosomes as determined by anti-Rab11+ immunostaining (26%–47%, Figure 3 C, Table 1), followed in descending order of accumulation by LAM 1+ lysosomes (11%–35%, Figure 3D, Table 1), Rab 7+ late endosomes (10%–30%, Figure 3B, Table 1), and to a lesser degree in EEA1+ early endosomes (5%–13%, Figure 3A, Table 1). Preferential compartmentalization of nanoparticles within recycling endosomes and lysosomes is consistent with previous reports for intracellular distribution of nanoformulated antiretroviral drugs and HIV-1 in human macrophages [29].

Release—Inflammatory cells are known to shed small vesicles (exosomes), which play a key role in intercellular communication [30]. Regarding macrophage-mediated delivery system, we reported that nanozyme is transferred to target cells along with carrier cells components including proteins and/or lipids [15]. Taken together, we hypothesized that macrophages emit and/or transfer exosomes with encapsulated nanozyme to recipient cells. To test this hypothesis, murine macrophages were preloaded with nanozyme, washed, and supplemented with fresh media. Released exosomes were isolated and tested for catalase activity. Significant enzymatic activity of catalase was detected in exosomal fraction (20,000 U/mL). Notably, in contrast to exosome-incorporated nanozyme, freshly prepared nanozyme did not precipitate under these isolation conditions. TEM images revealed exosomes with encapsulated nanozyme (Figure 4A).

Next, we reported nanozyme transport to contiguous target cells through bridging conduits (BC), filopodia and elongated lamellipodia [15]. To this end, we examined nanozyme colocalization with actin microfilaments, the main cytoskeleton components forming BC in macrophages (Figure 4 C and D, Table 1). A remarkable effect of macrophage activation on nanozyme intracellular localization was found within the carrier cells. Little overlap of nanozyme and actin staining was demonstrated in non-activated macrophages (26%, Figure 4C, Table 1); contrastingly, in lipopolysaccharide (LPS)- and interferon gamma (IFN-γ)-activated macrophages nanozyme was relocated to BC (61%, Figure 4D, Table 1). This was

consistent with significant decrease in retained, and increase in released from macrophages nanozyme upon activation (Figure 4B), suggesting a triggered mechanism of nanozyme release from the carrier cells at the inflammation site.

II. Receiver cells: Nanozyme Entrance and Intracellular Trafficking in Neurons and Human Brain Microvessel Endothelial Cells (HBMEC)

Internalization—We reported earlier that facilitated transport of the nanozyme from macrophages to endothelial and neural target cells occurred through endocytosis-independent mechanisms that involved fusion of cellular membranes of the donor and receiver cells; wrapping of nanozyme into lipid coatings from the donor cell; and development of macrophage bridging conduits and transport of nanozyme through microtubules in macrophages [15]. Here we further elucidated mechanism of these processes: i) release of nanozyme incorporated in exosomes from macrophages into extracellular media; and ii) nanozyme transfer from macrophages to receiver cells through BC, filopodia and lamellipodia.

To investigate the first pathway, murine macrophages were preloaded with fluorescently-labeled nanozyme, washed, and supplemented with fresh media. Exosomes with encapsulated nanozyme released to extracellular media from macrophages were harvested and purified. Then, the isolated exosomal fraction was added to CATH.a neurons and the dynamics of nanozyme accumulation within target cells were visualized by confocal microscopy (Figure 5, Media S1). Images clearly demonstrated exosomes with encapsulated nanozyme adsorbing on the surface of the recipient cells (Figure 5, arrowheads), and fusing with the cellular membranes. Release of nanozyme into the cytoplasm of neurons resulted in a diffuse fluorescent staining. We hypothesized that nanozyme incorporation into exosomes improved drug binding with lipid membranes of the target cells. Adhered to the plasma membranes exosomes fuse with them and discharge their cargo into target cells.

Furthermore, we evaluated intracellular trafficking of transported from macrophages nanozyme in the receiver cells. Corroborative evidence of concurrent transfer of nanozyme in exosomes was obtained when plasma membranes of macrophages preloaded with fluorescently-labeled nanozyme were stained with antibody to CD14, and then added to recipient human brain microvessel endothelial cells (HBMEC). Confocal microscopy revealed vesicle-like inclusions with macrophages membranes staining (green) colocalized with fluorescently-labeled nanozyme (red) in recipient HBMEC that was manifested in yellow color (Figure 6A, arrowheads). This suggests that loaded in the carrier cells nanozyme was incorporated into lipid-consisting vesicles, exosomes, and then transported along with them into receiver cells.

Next, evaluation of intracellular trafficking of nanozyme in the receiver cells revealed substantial colocalization of nanozyme with tubulin in HBMEC (45%–58%, Figure 6B, Table 2) suggesting that these components of the cytoskeleton might be used as tracts for nanozyme transport in the receiver cells. Interestingly, contrary to carrier cells, the involvement of actin microfilaments in nanozyme transport was minimally detected in the recipient cells (13%–19%, Figure 6C, Table 2).

Regarding the second pathway of nanozyme transfer through BC, the role of actual contact between carrier and recipient cells was investigated. The two, left (**A**) and right (**B**) inserts on Figure 7 represent sections of the confocal image at higher magnification taken from the close (**A**) or distant (**B**) to the donor-receiver contact site. Confocal microphotographs revealed initial localized distribution of nanozyme in the recipient cells at the sites of their contact with the donor human macrophages (Figure 7A). At the same time, sites distant from

the cell-cell contact points showed substantially less nanozyme accumulation (Figure 7B), signifying a crucial role of cell-to-cell contact in this transfer.

As Gap junction channels formed by protein subunits, connexins, are conduits for the direct cell-to-cell exchange of various molecules [31] between the cytoplasm of two cells, we examined whether nanozyme transfer occurs through this pathway by inhibiting connexin 43 gap junction intercellular communications with the phorbol ester, 12-O-tetradecanoylphorbol-13-acetate (PMA) [32]. Preloaded with nanozyme, murine macrophages were divided into two groups and incubated with CATH.a neurons in the presence or absence of PMA. No significant effect of gap junction assembly inhibition on nanozyme accumulation in the receiver cells was found (Table S2), suggesting a gap junction-independent pathway of nanozyme entry, probably due to the relatively large particle size and nanozyme inclusion in exosomes.

Intracellular trafficking—Intracellular localization of macrophage-derived and transferred nanozyme was examined and compared with the distribution of cell-free nanozyme in target HBMEC (Figure 8) and CATH.a neurons (Figure 9). Major differences in the accumulation levels and trafficking of nanozyme were observed for cell-derived and cell-free nanozyme. First, the amount of nanozyme transferred from macrophages to target endothelial cells and neurons (Figures 8 and 9, **Set I**) was substantially greater than that from free nanozyme (Figures 8 and 9, **Set II**), which is consistent with our previous report [15]. Second, nanozyme transferred from macrophages diffused throughout the entire target cell demonstrating strong colocalization with endosomal compartments (especially, late and recycling endosomes, and lysosomes) as well as mitochondria, and ER (Figure 8, **Set I,** Table 2). Notably, the considerable colocalization with the late endosomal marker, Rab 7, might in part be due to the expression of this protein in exosomes containing nanozyme that were shed from macrophages and then internalized into HBMEC [33]. In contrast, free nanozyme was localized mostly in early endosomes and then sorted to lysosomal compartments (Figure 8, **Set II,** Table 2). Important differences in intracellular localization reflect rather unique trafficking of nanozyme from macrophages to target cells than greater accumulation levels. Thus, similar restricted localization of free nanozyme in lysosomal compartments was demonstrated when HBMEC were incubated with a four-fold higher concentration of nanozyme in the media (Figure S4).

III. Therapeutics

Facilitated nanozyme access to target endothelial cells compared to free nanozyme might result in the greater BBB transport and consequently improved therapeutic effect. Accordingly, levels of nanozyme accumulation in HBMEC transferred from carrier cells or from the media were assessed by FACS. Indeed, significantly greater accumulation levels of macrophage-mediated nanozyme transfer compared to free nanoparticles were demonstrated (Figure 10A).

Furthermore, given the increased nanozyme transport from murine macrophages to CATH.a neurons and the efficient ROS elimination when compared to free nanozyme [15], we hypothesized that cell-derived nanozyme may increase neuronal survival upon oxidative stress. To test this hypothesis, the effect of nanozyme-loaded murine macrophages on neuronal survival was evaluated with 6-hydroxydopamine (6-OHDA)-treated CATH.a, an *in vitro* model which recapitulates components of PD neurodegeneration. Nanozyme loaded in murine macrophages has greater neuroprotective activity than the identical concentrations of free enzyme (Figure 10B), probably, due to the greater nanozyme intracellular levels as well as diffused intracellular distribution with favorable access to mitochondria in the target neuronal cells.

DISCUSSION

Macrophage-mediated transfer of nanoformulated catalase to endothelial cells and neurons permits highly efficient drug delivery [13, 15, 34]. Notably, this activity is not specific for nanozymes but can apply to other nanoparticles therapeutic systems. Thus, transfer of gold nanoparticles with the same size as the nanozyme (~60 nm) and PEG corona from preloaded murine macrophages (Figure S5A) to adjacent CATH.a neurons (Figure S5B) was demonstrated by TEM. Interesting, nanoparticles transferred from macrophages were localized largely in the cytoplasm of contacted neurons (Figure S5 B). In contrast, nanoparticles accumulated from the media were localized in endocytic vesicles (Figure S5 C). Until now, it was not clear how cell based drug carriers improve disease outcomes from nanoparticles administered alone. Herein, we uncovered intracellular trafficking of nanozyme from macrophages to neurons and brain microvessel endothelial cells that are intimately involved with one another and in the pathobiology of neurodegenerative disorders.

There are several requirements for successful cell-based drug carriage. *First*, drug nanoparticles should exploit intracellular entry and trafficking routes that avoid their rapid degradation. Macrophages have evolved a variety of strategies to internalize pathogens, particles and solutes. Each can enter through a range of mechanisms that include phagocytosis, receptor-mediated endocytosis, and pinocytosis [24]. Pinocytosis and receptor-mediated endocytosis share clathrin-based mechanisms and can readily occur independently of actin polymerization. By contrast, phagocytosis occurs through cell uptake of larger particles (>0.5 μm) by a clathrin-independent mechanism and targets degradation into lysosomes. In the current works nanozymes entered macrophages principally through clathrin-coated pits consistent with what was found recently by nanoformulated antiretroviral drugs in human macrophages [29]. Accordingly, inhibition of pinocytosis and macropinocytosis diminish nanozyme accumulation, contrary to the luck of the effect of phagocytosis inhibition.

Clathrin-coated vesicles containing nanozyme undergo fusion with early sorting endosomes following downstream sorting to late and recycling endosomes, and lysosomes. Colocalization of particles with the ER and mitochondria was limited. The predominant accumulation of nanozyme in recycling endosomes over lysosomes support the preservation of catalase enzymatic activity against degradation in carrier cells and its substantial extracellular release or into adjacent target cells. Noteworthy, a buffering effect of nanozyme that increases lysosomal pH as previously reported [14] provides additional preservation of catalase. As a result, such trafficking provides for non-degraded cargoes that carry functionally-active enzymes capable of biologic responses during disease.

Release of nanozyme from macrophages occurs through BC with the engagement of actin microfilaments. Importantly, activation of macrophages with LPS and IFN-γ that reflect, in part, the inflammatory environment during progressive neurodegenerative diseases, resulted in nanozyme relocation from endocytic compartments into the BC, thus supporting the triggered release of nanozyme at the sites of active inflammation.

Intercellular exchange of organelles and proteins is also a known mechanism of cell communication [29, 35–37]. Indeed, HIV-1 spreads from infected to uninfected cells through BC and endocytic trafficking [29, 38]. Following entry, a portion of HIV-1 constituents are sorted into non-degrading endocytic compartments (early and recycling endosomes), then shuttled through nanotubes to uninfected cells. Herein, we examined whether the same trafficking mechanism is involved in macrophage-mediated nanozyme transfer to neighboring cells. Besides BC development, macrophages constitutively secrete

small vesicles, exosomes, affecting the physiology of neighboring recipient cells that acquire new receptors, enzymes or genetic material [30, 39]. We reported the co-transport of nanozyme and lipids from macrophages into brain microvessel endothelial and neuronal targets [15]. We hypothesized that nanozyme transfers from macrophages via exosomes facilitates plasma membrane penetration and orchestrates nanozyme intracellular trafficking in recipient cells. Indeed, the mechanism of cell-derived nanozyme entry and intracellular trafficking in adjacent target cells differs from the uptake of cell-free nanoparticles in divergent ways. *First*, levels of nanozyme accumulated from macrophages to brain microvessel endothelial and neural cells were greater than the amount of cell-free nanozyme accumulated from the media. *Second*, confocal images demonstrate diffuse distribution of nanozyme transferred from macrophages, in contrast to cell-free nanozyme localized in endosomal compartments, mainly in lysosomes and early endosomes. This might be due to encapsulation of nanozyme into exosomes from carrier cells that allows their efficient fusion with plasma membranes of target cells and stable intracellular localization. Given strong colocalization of nanozyme with tubulin microfilaments in microvessel endothelial cells, we hypothesized that exosomes with incorporated nanozyme travel from macrophages to target cells alongside tubulin tracts. This mechanism enables them to reach different intracellular compartments such as mitochondria, cytoplasm, and ER, where ROS may be efficiently deactivated as no involvement of gap junction channels in this transfer was found (Figure 11).

We posit that unique nanozyme trafficking from nanozyme carrier cells plays a key role in the therapeutic effects of the enzyme in recipient cells. Indeed, increased neuronal survival in the presence of nanozyme-loaded murine macrophages demonstrated significant improvements against oxidative stress compared to cell-free nanozyme. In addition, association of enzymes with lipid bilayers (*e.g.*, the surface of liposomes) was demonstrated to improve their stability and resistance to inactivation at low pH or high concentration of H_2O_2 [40]. A similar stabilization effect might take place upon incorporation of nanozyme into exosomes. Furthermore, macrophages loaded with nanozyme promote its accumulation in brain microvessel endothelial cells, which in addition may improve its transport across the BBB. In fact, this study suggests that macrophages can provide a shuttle service to facilitate transport of therapeutic proteins that hitch hike onto the cells to the disease sites.

Any drug delivery system needs to be efficient, safe, and limit secondary tissue toxicities. We previously demonstrated that using cells as delivery vehicles enables targeted drug transport, and prolonged circulation times, along with minimizing systemic adverse effects with targeted delivery [12, 13, 34]. The current study revealed mechanisms for these effects on a cellular level indicating for the first time that macrophages improve entry and intracellular drug distribution in target cells (Figure 11) resulting in superior therapeutic effect. Furthermore, better understanding of macrophage-mediated facilitated transfer mechanisms allows utilizing this system more efficiently. In particular, activation of macrophages with specific agents may significantly improve ability of exosomes to adhere and fuse with the cellular membranes of the target cells, and therefore, enhance the therapeutic effect of the drug formulation. Finally, an ideal drug nanocarrier for cell-mediated delivery should target specific intracellular pathways and compartments, for example, recycling endosomes in the cell carriers, mitochondria and cytoplasm in neurons, or endosomes involved in transcytosis within brain microvessel endothelial cells. Such drug particle trafficking would ultimately increase the therapeutic index and improve disease outcomes.

FUTURE PERSPECTIVE

Using macrophages for drug delivery enables targeted drug transport, and prolonged circulation times, along with reductions in cell and tissue toxicities. The cells migrate across impermeable barriers and can release drug cargo at sites of infection or tissue injury. In addition, these cells are capable of cell-to-cell transmission of drug-laden nanoparticles improving their therapeutic outcomes. Indeed, there are several limitations related to the efficient drug loading in cell carriers, triggered release, ability of macrophages to reach the damaged region of the brain in meaningful levels, as well as efficient protection of the drug inside the cells-carriers against degradation. Nevertheless, our data indicate that choosing a right formulation for a drug, along with an optimal cell-carrier can accomplish these goals. Such systems for drug carriage and targeted release represent a novel disease combating strategy being applied to a spectrum of human disorders.

EXECUTIVE SUMMARY

- **Overall Summary.** Drug-carrier cells, macrophages, support transfer of nanoformulated catalase, “nanozyme”, to adjacent brain microvessel endothelial cells and neurons by endocytosis-independent mechanisms. The transported nanozyme showed diffused intracellular distribution throughout the recipient cells in contrast to macrophage-free nanozymes that were localized in lysosomes following endocytic entry.
- **Cell Carriers: Nanozyme Entry and Intracellular Trafficking in Macrophages.** Nanozyme enters to macrophages mainly in clathrin-coated vesicles that undergo fusion with early sorting endosomes following downstream sorting to late and recycling endosomes. This supports the preservation of catalase enzymatic activity against degradation in carrier cells and its substantial extracellular release or into adjacent target cells.
- **Cell Carriers: Release**. Triggered by inflammatory signals release of nanozyme from macrophages occurs through bridging conduits with the engagement of actin microfilaments.
- **Receiver cells: Nanozyme Entrance and Intracellular Trafficking.** Nanozyme transfer from macrophages via exosomes facilitates plasma membrane penetration and orchestrates nanozyme intracellular trafficking in recipient cells.
- **Therapeutics.** A unique nanozyme trafficking from nanozyme carrier cells facilitate neuroprotective responses and can improve clinical outcomes for neurodegenerative diseases.

Supplementary Material

Refer to Web version on PubMed Central for supplementary material.

Acknowledgments

This study was supported by the National Institutes of Health grants 1R01 NS057748 (to EVB), 2R01 NS034239, 2R37 NS36126, P01 NS31492, P20RR 15635, P01 MH64570, P01 NS43985 (to HEG), RR021937 (to AVK), 1R01 NS070190 (to RLM), 1R01 MH081780 (to GDK), and Russian Ministry of Science and Education grants 02.740.11.5231 and 11.G34.31.0004 (to AVK and NLK). We are grateful to Janice A. Taylor and James R. Talaska

(Confocal Laser Scanning Microscope Core Facility, UNMC) for providing assistance with confocal microscopy and the Nebraska Research Initiative. We also gratefully acknowledge Tom W. Bargar for assistance in electron microscopic imaging.

REFERENCES

1. Mcgeer PL, Itagaki S, Boyes BE, et al. Reactive microglia are positive for hla-dr in the substantia nigra of parkinson's and alzheimer's disease brains. Neurology. 1988; 38(8):1285–1291. [PubMed: 3399080]
2. Busciglio J, Yankner BA. Apoptosis and increased generation of reactive oxygen species in down's syndrome neurons in vitro. Nature. 1995; 378(6559):776–779. [PubMed: 8524410]
3. Ebadi M, Srinivasan SK, Baxi MD. Oxidative stress and antioxidant therapy in parkinson's disease. Prog Neurobiol. 1996; 48(1):1–19. [PubMed: 8830346]
4. Wu DC, Teismann P, Tieu K, et al. Nadph oxidase mediates oxidative stress in the 1-methyl-4-phenyl-1,2,3,6-tetrahydropyridine model of parkinson's disease. Proc Natl Acad Sci U S A. 2003; 100(10):6145–6150. [PubMed: 12721370]
5. Arends MJ, Wyllie AH. Apoptosis: Mechanisms and roles in pathology. Int Rev Exp Pathol. 1991; 32:223–254. [PubMed: 1677933]
6. Chan PH. Reactive oxygen radicals in signaling and damage in the ischemic brain. J Cereb Blood Flow Metab. 2001; 21(1):2–14. [PubMed: 11149664]
7. Ambani LM, Van Woert MH, Murphy S. Brain peroxidase and catalase in Parkinson disease. Arch Neurol. 1975; 32(2):114–118. [PubMed: 1122174]
8. Riederer P, Sofic E, Rausch WD, et al. Transition metals, ferritin, glutathione, and ascorbic acid in parkinsonian brains. J Neurochem. 1989; 52(2):515–520. [PubMed: 2911028]
9. Abraham S, Soundararajan CC, Vivekanandhan S, et al. Erythrocyte antioxidant enzymes in parkinson's disease. Indian J Med Res. 2005; 121(2):111–115. [PubMed: 15756044]
10. Gonzalez-Polo RA, Soler G, Rodriguezmartin A, et al. Protection against mpp+ neurotoxicity in cerebellar granule cells by antioxidants. Cell Biol Int. 2004; 28(5):373–380. [PubMed: 15193280]
11. Pappert EJ, Tangney CC, Goetz CG, et al. Alpha-tocopherol in the ventricular cerebrospinal fluid of parkinson's disease patients: Dose-response study and correlations with plasma levels. Neurology. 1996; 47(4):1037–1042. [PubMed: 8857741]
12. Batrakova EV, Li S, Reynolds AD, et al. A macrophage-nanozyme delivery system for parkinson's disease. Bioconjug Chem. 2007; 18(5):1498–1506. [PubMed: 17760417] *of interest: This manuscript reported development and characterization of cell-mediated delivery system of antioxidant enzyme, catalase. Loading, release, and protection of enzymatic activity of catalase in bone marrow-derived monocytes (BMM) are evaluated in *in vitro* model of PD.
13. Brynskikh AM, Zhao Y, Mosley RL, et al. Macrophage delivery of therapeutic nanozymes in a murine model of parkinson's disease. Nanomedicine (Lond). 2010; 5(3):379–396. [PubMed: 20394532] **of considerable interest: This study supports the feasibility of cell-mediated drug delivery to the brain by examining i) the nanozyme loading capacity for cell carriers; ii) the effect of nanozymes on cell viability and function; and iii) the neuroprotective activities of BMM-carried nanozyme against MPTP intoxication in *in vivo* model of PD.
14. Zhao Y, Haney MJ, Klyachko NL, et al. Polyelectrolyte complex optimization for macrophage delivery of redox enzyme nanoparticles. Nanomedicine (Lond). 2011; 6(1):25–42. [PubMed: 21182416] *of interest: This manuscript reported optimization of nanozyme structure for high loading capacity and release from the cell-carriers along with the best protection of catalase activity.
15. Haney MJ, Zhao Y, Li S, et al. Cell-mediated transfer of catalase nanoparticles from macrophages to brain endothelial, glial and neuronal cells. Nanomedicine (Lond). 2011 **of considerable interest: This is the first demonstration that loaded macrophages discharge nanoformulated drug into target cells that may be beneficial for therapy of PD.
16. Vinogradov S, Bronich T, Kabanov A. Self-assembly of polyamine-poly(ethylene glycol) copolymers with phosphorothioate oligonucleotides. Bioconjugate Chemistry. 1998; 9(6):805–812. [PubMed: 9815175]

17. Dou H, Destache CJ, Morehead JR, et al. Development of a macrophage-based nanoparticle platform for antiretroviral drug delivery. Blood. 2006; 108(8):2827–2835. [PubMed: 16809617]
18. Srtevenson, HC.; Fauci, AS. Purification of human monocytes by counter-current centrifugation elutriation. New York: Marcel Decker Press; 1981.
19. Batrakova EV, Vinogradov SV, Robinson SM, et al. Polypeptide point modifications with fatty acid and amphiphilic block copolymers for enhanced brain delivery. Bioconjug Chem. 2005; 16(4):793–802. [PubMed: 16029020]
20. Rasband WS. Imagej. 1997–2007
21. Bolte S, Cordelieres FP. A guided tour into subcellular colocalization analysis in light microscopy. J Microsc. 2006; 224(Pt 3):213–232. [PubMed: 17210054]
22. Batrakova E, Han H, Miller D, et al. Effects of pluronic p85 unimers and micelles on drug permeability in polarized bbmec and caco-2 cells. Pharm Res. 1998; 15(10):1525–1532. [PubMed: 9794493]
23. Sahay G, Alakhova DY, Kabanov AV. Endocytosis of nanomedicines. J Control Release. 2010; 145(3):182–195. [PubMed: 20226220]
24. Aderem A, Underhill DM. Mechanisms of phagocytosis in macrophages. Annu Rev Immunol. 1999; 17:593–623. [PubMed: 10358769]
25. Lunov O, Zablotskii V, Syrovets T, et al. Modeling receptor-mediated endocytosis of polymer-functionalized iron oxide nanoparticles by human macrophages. Biomaterials. 32(2):547–555. [PubMed: 20880574]
26. Rappoport JZ. Focusing on clathrin-mediated endocytosis. Biochem J. 2008; 412(3):415–423. [PubMed: 18498251]
27. Sahay G, Batrakova EV, Kabanov AV. Different internalization pathways of polymeric micelles and unimers and their effects on vesicular transport. Bioconjug Chem. 2008; 19(10):2023–2029. [PubMed: 18729494]
28. Freundt EC, Czapiga M, Lenardo MJ. Photoconversion of lysotracker red to a green fluorescent molecule. Cell Res. 2007; 17(11):956–958. [PubMed: 17893709]
29. Kadiu I, Gendelman HE. Macrophage endocytic trafficking networks facilitate hiv-1 intercellular transport through tunneling nanotubes: A novel pathway for viral dissemination. The Journal of Molecular Medicine in revision. 2011
30. Thery C, Ostrowski M, Segura E. Membrane vesicles as conveyors of immune responses. Nat Rev Immunol. 2009; 9(8):581–593. [PubMed: 19498381]
31. Simon AM, Goodenough DA. Diverse functions of vertebrate gap junctions. Trends Cell Biol. 1998; 8(12):477–483. [PubMed: 9861669]
32. Murray AW, Fitzgerald DJ. Tumor promoters inhibit metabolic cooperation in cocultures of epidermal and 3t3 cells. Biochem Biophys Res Commun. 1979; 91(2):395–401. [PubMed: 518638]
33. Almqvist N, Lonnqvist A, Hultkrantz S, et al. Serum-derived exosomes from antigen-fed mice prevent allergic sensitization in a model of allergic asthma. Immunology. 2008; 125(1):21–27. [PubMed: 18355242]
34. Batrakova EV, Gendelman HE, Kabanov AV. Cell-mediated drug delivery. Expert Opin Drug Deliv. 2011; 8(4):415–433. [PubMed: 21348773]
35. Onfelt B, Nedvetzki S, Benninger RK, et al. Structurally distinct membrane nanotubes between human macrophages support long-distance vesicular traffic or surfing of bacteria. J Immunol. 2006; 177(12):8476–8483. [PubMed: 17142745]
36. Sherer NM, Lehmann MJ, Jimenez-Soto LF, et al. Retroviruses can establish filopodial bridges for efficient cell-to-cell transmission. Nat Cell Biol. 2007; 9(3):310–315. [PubMed: 17293854]
37. Chinnery HR, Pearlman E, Mcmenamin PG. Cutting edge: Membrane nanotubes in vivo: A feature of mhc class ii+ cells in the mouse cornea. J Immunol. 2008; 180(9):5779–5783. [PubMed: 18424694]
38. Kadiu I, Ricardo-Dukelow M, Ciborowski P, et al. Cytoskeletal protein transformation in hiv-1-infected macrophage giant cells. J Immunol. 2007; 178(10):6404–6415. [PubMed: 17475870]

39. Bhatnagar S, Shinagawa K, Castellino FJ, et al. Exosomes released from macrophages infected with intracellular pathogens stimulate a proinflammatory response in vitro and in vivo. Blood. 2007; 110(9):3234–3244. [PubMed: 17666571]

40. Nagami H, Yoshimoto N, Umakoshi H, et al. Liposome-assisted activity of superoxide dismutase under oxidative stress. J Biosci Bioeng. 2005; 99(4):423–428. [PubMed: 16233812]

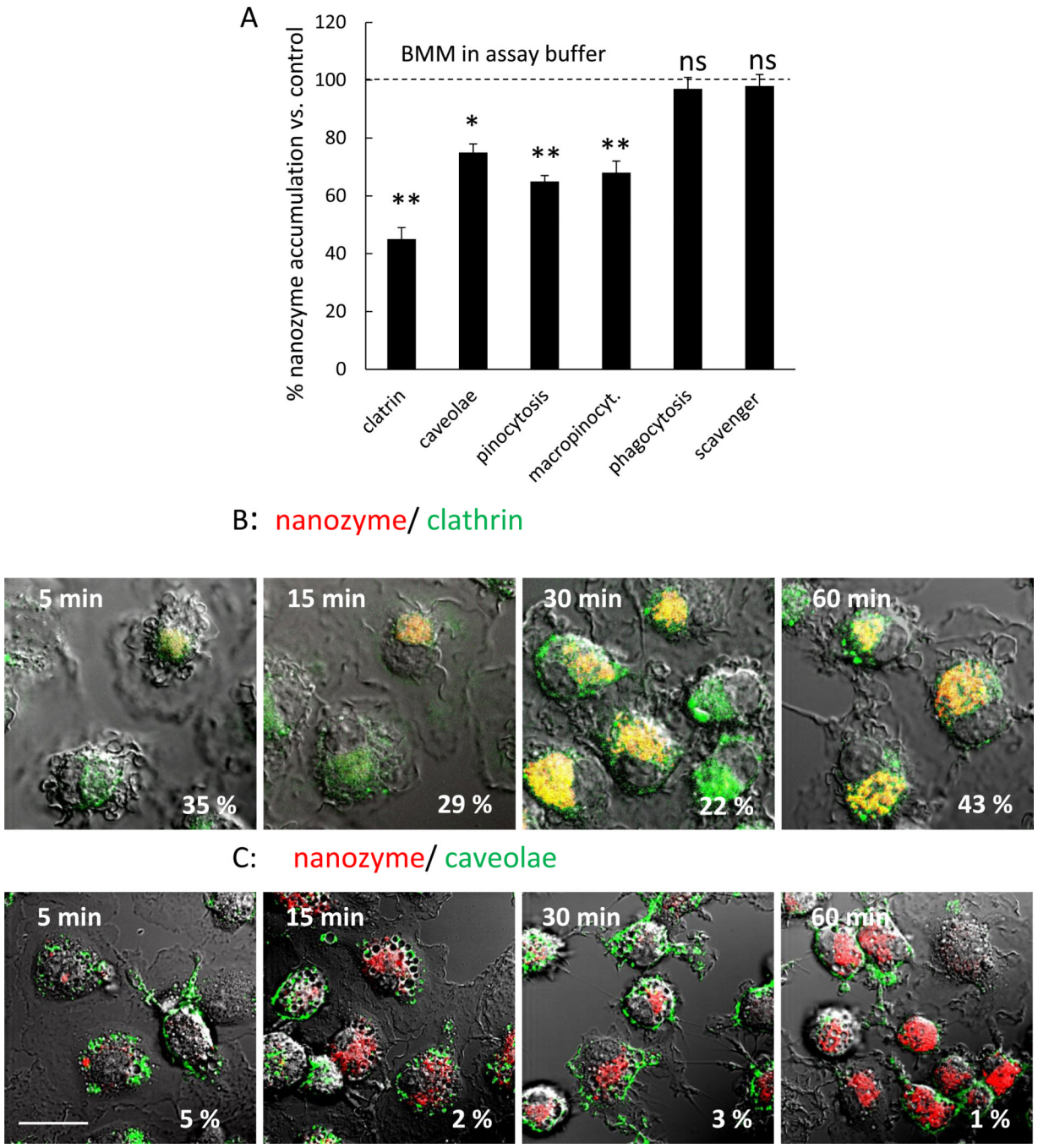

Figure 1. Nanozyme entry into Macrophage occurs through clathrin-coated pits and caveolae-mediated endocytosis

(**A**) Murine macrophages were exposed to fluorescently-labeled nanozyme in the presence or absence of various inhibitors for 1 hour, and nanozyme uptake was analyzed by fluorescence spectroscopy. (**B, C**) Murine macrophages were incubated for different times with Alexa Fluor-649-labeled nanozyme, stained with FITC-Tf (clathrin-mediated endocytosis marker, 25 μg/ml), or FITC-CTB (caveolae-mediated endocytosis marker, 25 μg/ml), and colocalization with nanozyme was evaluated by confocal microscopy. Refer also to Table 1 for quantative colocalization. Statistical significance of nanozyme uptake in the

presence of the inhibitors compared to murine macrophages in assay buffer is shown by asterisks (**) $p<0.005$. Data represent means ± SEM (N = 4). Bar = 20 μm.

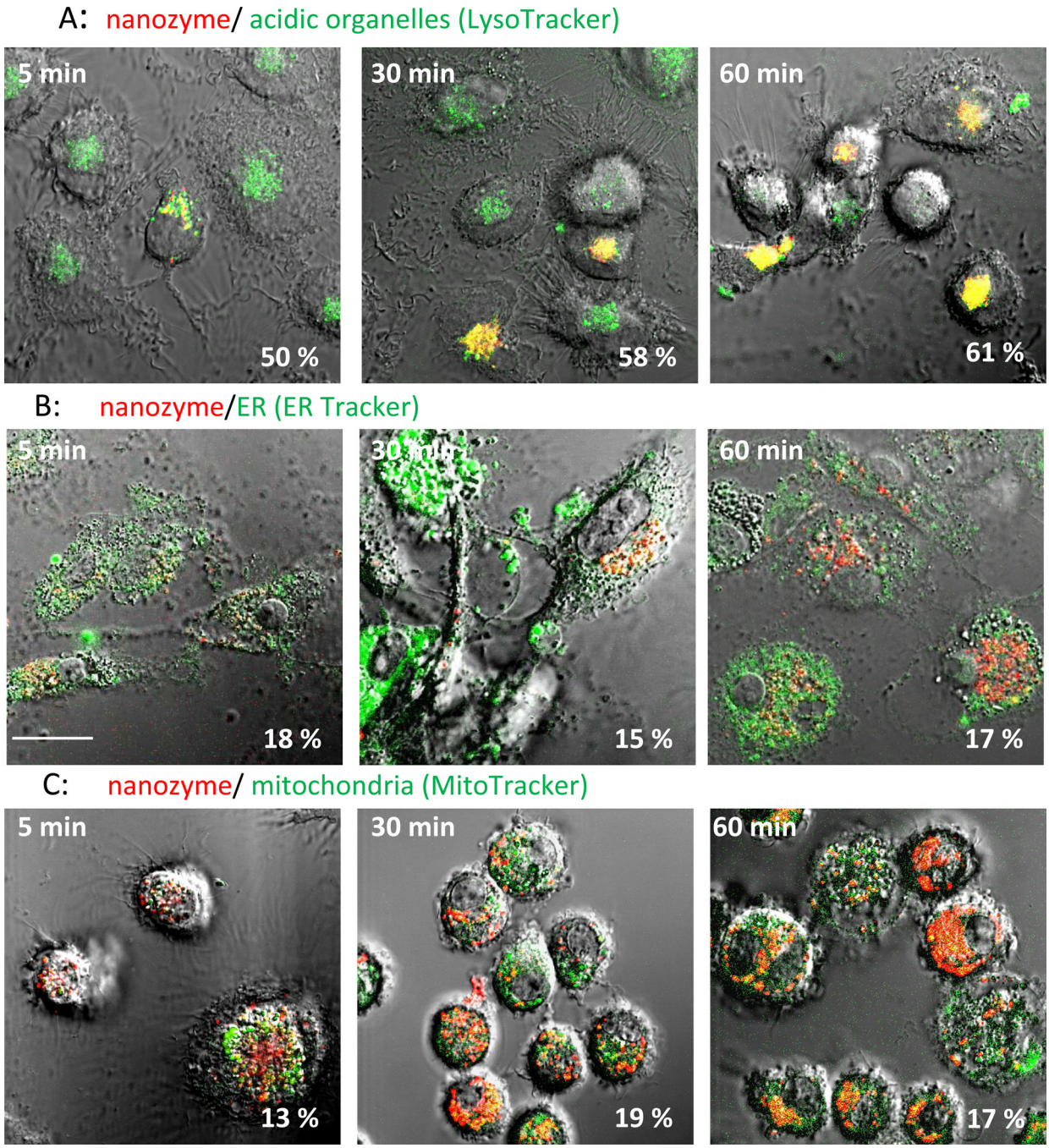

Figure 2. Nanozyme intracellular localization in live human macrophages

The cells were incubated with nanozyme for different times and stained with (**A**) LysoTracker Green (20 nM), (**B**) ERTracker Green (1 μM), or (**C**) MitoTracker Green (50 nM). Colocalization of nanozyme (red) and compartment staining (green) manifested in yellow. Nanozyme accumulated largely in acidified compartments, and at substantially lesser degree in ER and mitochondria. Refer also to Table 1 for quantative colocalization. Bar = 20 μm.

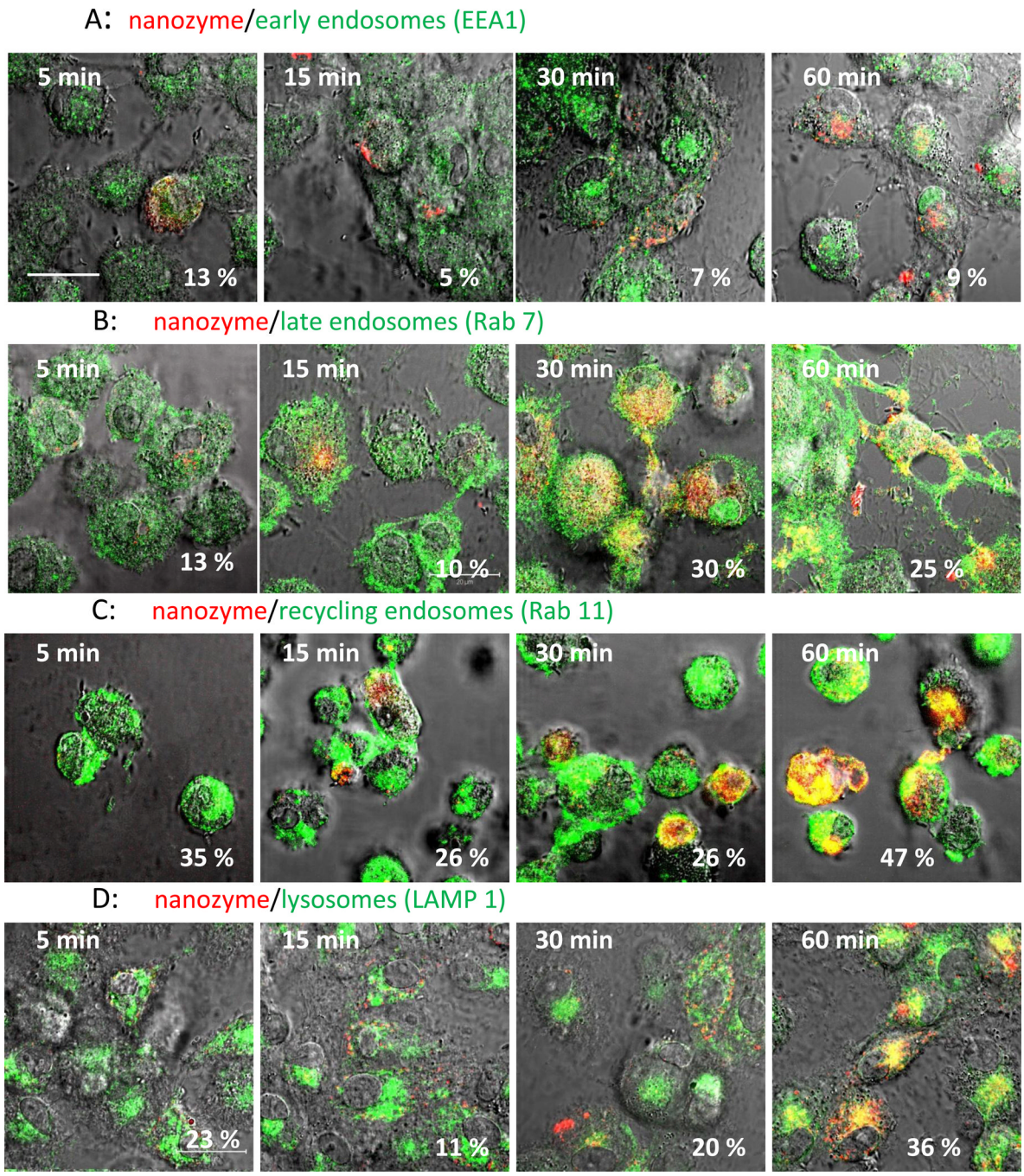

Figure 3. Localization of nanozyme in endosomal compartments in fixed human macrophages

Human monocyte-derived macrophages (HMDM) were incubated with nanozyme for different times, fixed, permeabilized, and stained with (**A**) FITC-conjugated EEA1 monoclonal antibody (to early endosomes), (**B**) mouse monoclonal antibody Rab7 (late endosomes), (**C**) mouse monoclonal antibody Rab11 (recycling endosomes), or (**D**) FITC-conjugated LAMP 1 monoclonal antibody (to lysosomes). In case of non-labeled primary mouse antibody (**B, C**), cells were further stained with FITC-conjugated secondary goat anti-mouse immunoglobulin G. Colocalization of nanozyme (red) and compartment staining

(green) manifested in yellow. Refer also to Table 1 for quantative colocalization. Bar = 20 μm.

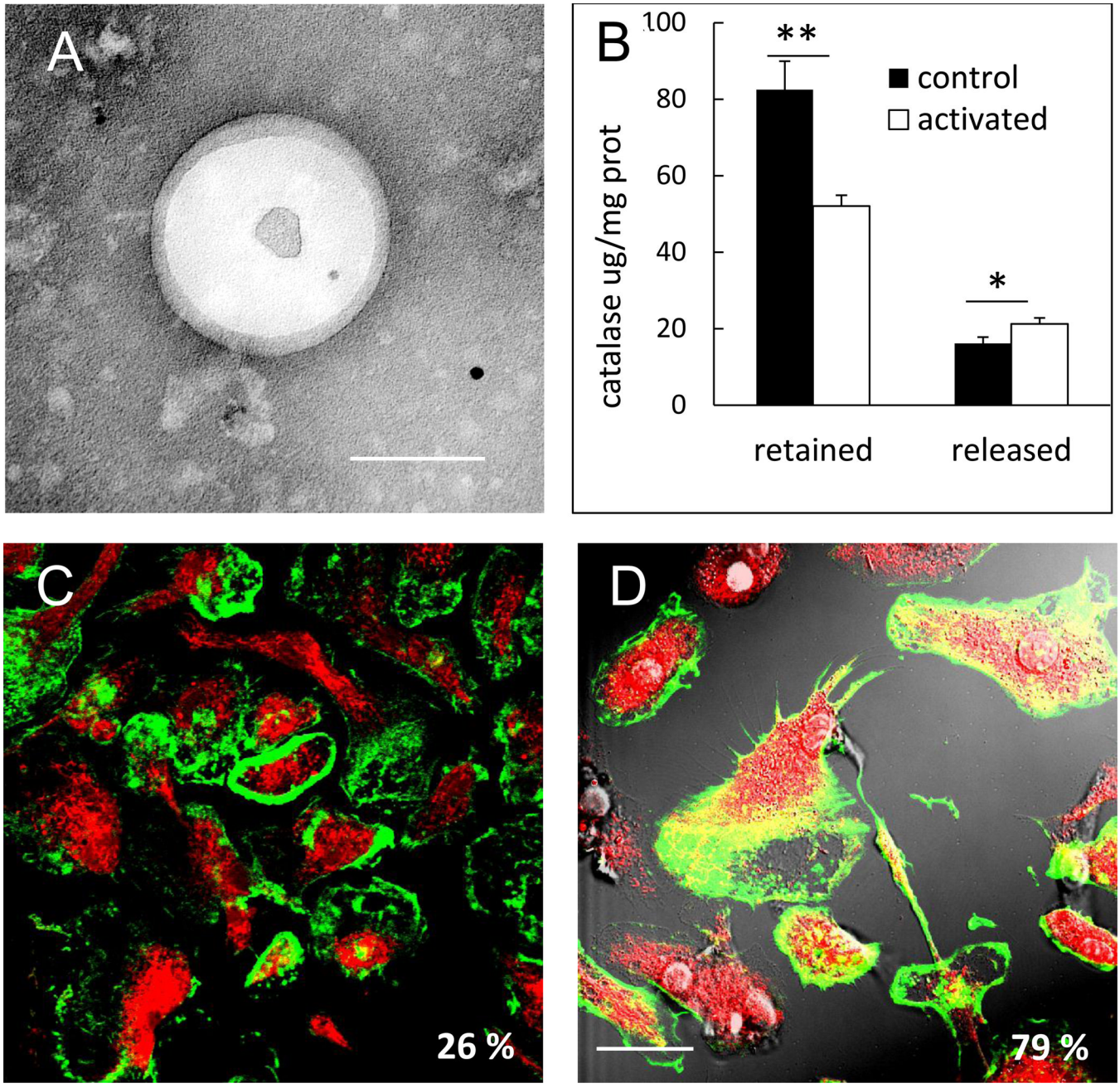

Figure 4. Release of nanozyme from macrophages in exosomes through BCs

Murine macrophages were loaded with nanozyme for one hour, washed, cultured in fresh media and exosomes purified from media after cetrifugation. Exosomes with encapsulated nanozyme were visualized by TEM (**A**). Bar = 100 nm. Relocation of nanozyme into in BMM upon activation with 500 ng/ml LPS and 200 ng/ml IFN-γ was documented by confocal microscopy (**C, D**). Murine macrophages were loaded with Alexa Fluor-675-labeled nanozyme and stained with phalloidin-488 for actin microfilaments. No overlap of nanozyme with actin microfilaments in macrophages was found in non-activated macrophages (**C**). Substantial nanozyme relocation to BCs in macrophages (manifested in yellow staining) occurred upon activation (**D**). Bar = 20 μm. This was confirmed by the levels of nanozyme retained in macrophages and released into the media. Nanozyme was

quantified by fluorospectrophotometry (**B**). Refer also to Table 1 for quantative colocalization.

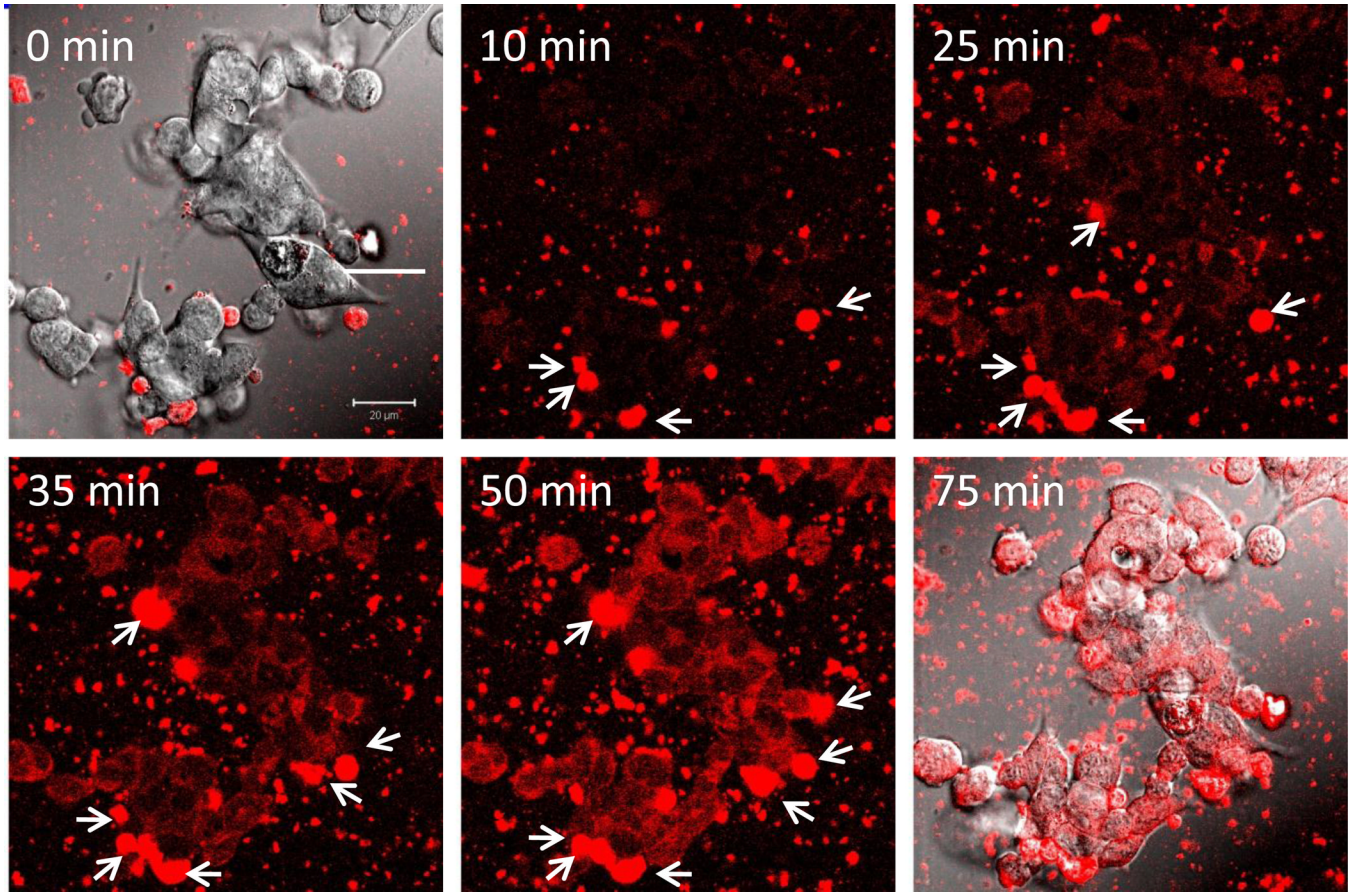

Figure 5. Dynamics and localization of nanozyme transported in exosomes from murine macrophages to CATH.a neurons

Confocal images of CATH.a neurons incubated with nanozyme (red)-containing exosomes released from preloaded murine macrophages. The first and last time fluorescence images are shown merged with differential interference contrast (DIC) microscopy. Exosomes in the media with encapsulated nanozyme were adsorbed on the surface of the recipient cells (shown by arrowheads) and fused with the membranes, releasing nanozyme into the cytoplasm of neurons that resulted in diffuse fluorescent staining. Bar = 20 μm.

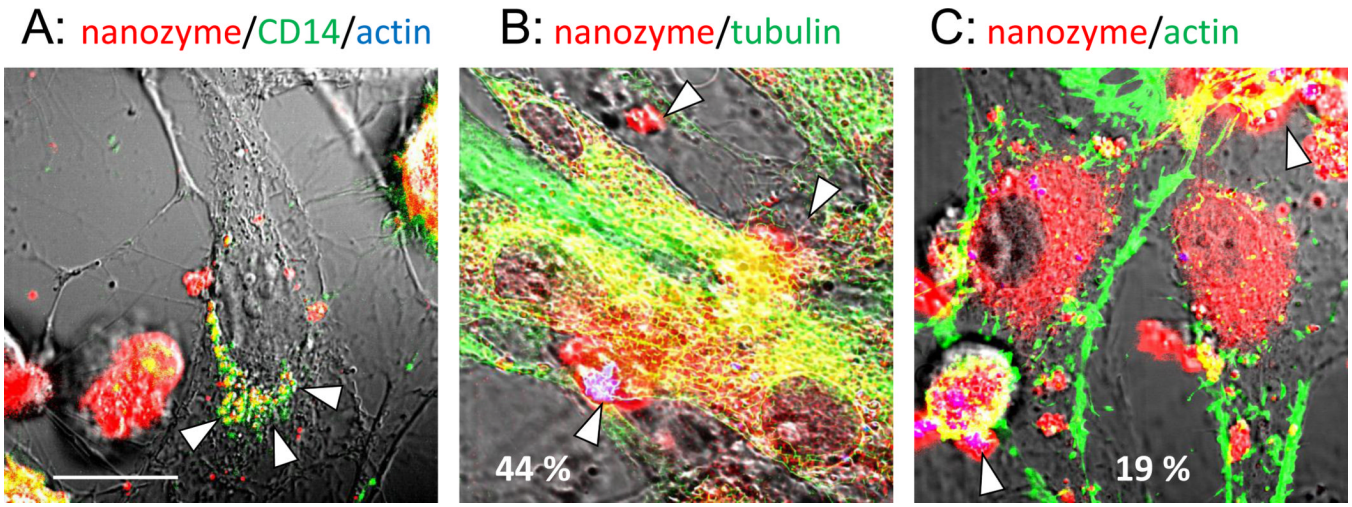

Figure 6. Nanozyme transfer from human macrophage exomes to HBMEC

HBMEC were incubated for one hour with human macrophages preloaded with nanozyme (red), fixed, permeabilized, and stained with anti-tubulin (green) (**B**), or phalloidin-488 to actin microfilaments (green) (**C**). In separate experiments, nanozyme-loaded macrophages were labeled with Alexa Fluor-488-anti-CD14 (green) (**A**) and then added to HBMEC. Images revealed substantial nanozyme colocalization in HBMEC with compartments from HMDM (**A**), and tubulin (**B**) (manifested in yellow) suggesting that nanozyme was transferred from carrier cells in exosomes alongside the tubulin microfilaments. Low colocalization of nanozyme with actin microfilaments was found in recipient cells (**C**). Exosomes from macrophages in HBMEC **(A)** and loaded macrophages **(B, C)** are shown by arrows. Bar represents 20 μm.

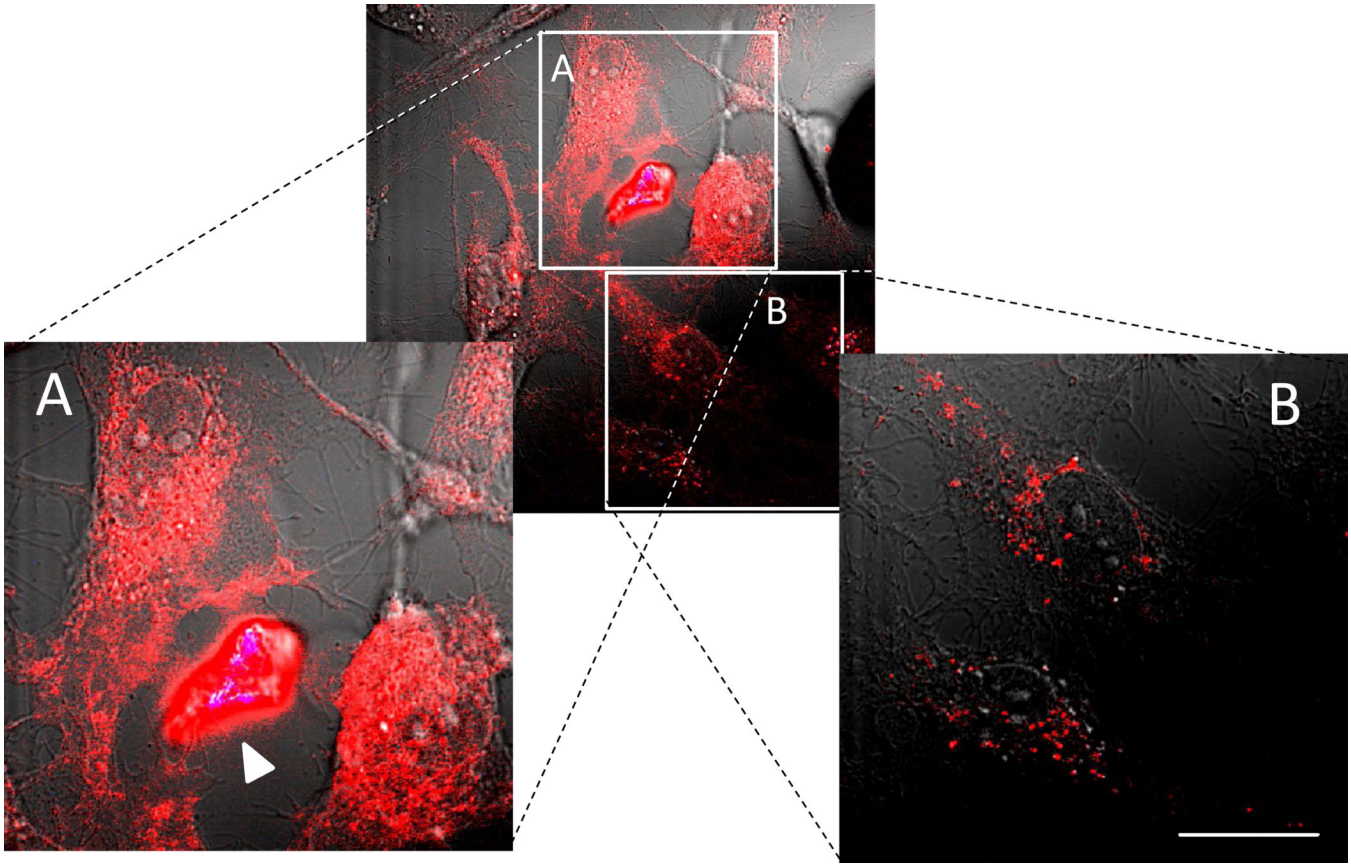

Figure 7. Nanozyme localized intracellular distribution in HBMEC transferred from the carrier cells, human macrophages

Human macrophages preloaded with fluorescently-labeled nanozyme were incubated with HBMEC for 30 min. Nanozyme was transferred to the receiver cells at the sites of cell-cell contact with the carrier cells (**A**) in contrast to low accumulation levels at the sites distant from the cell contact (**B**). Bar represents 20 μm.

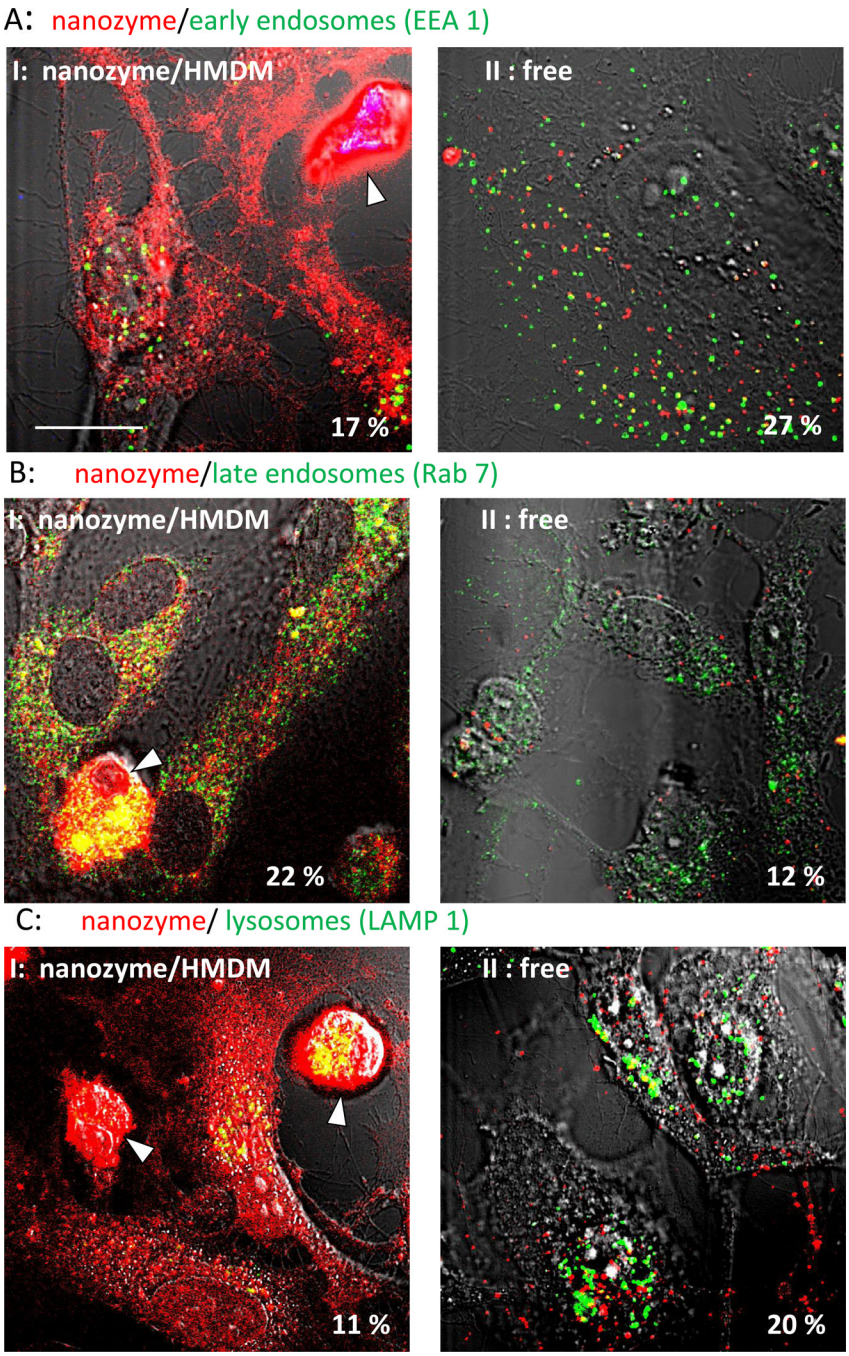

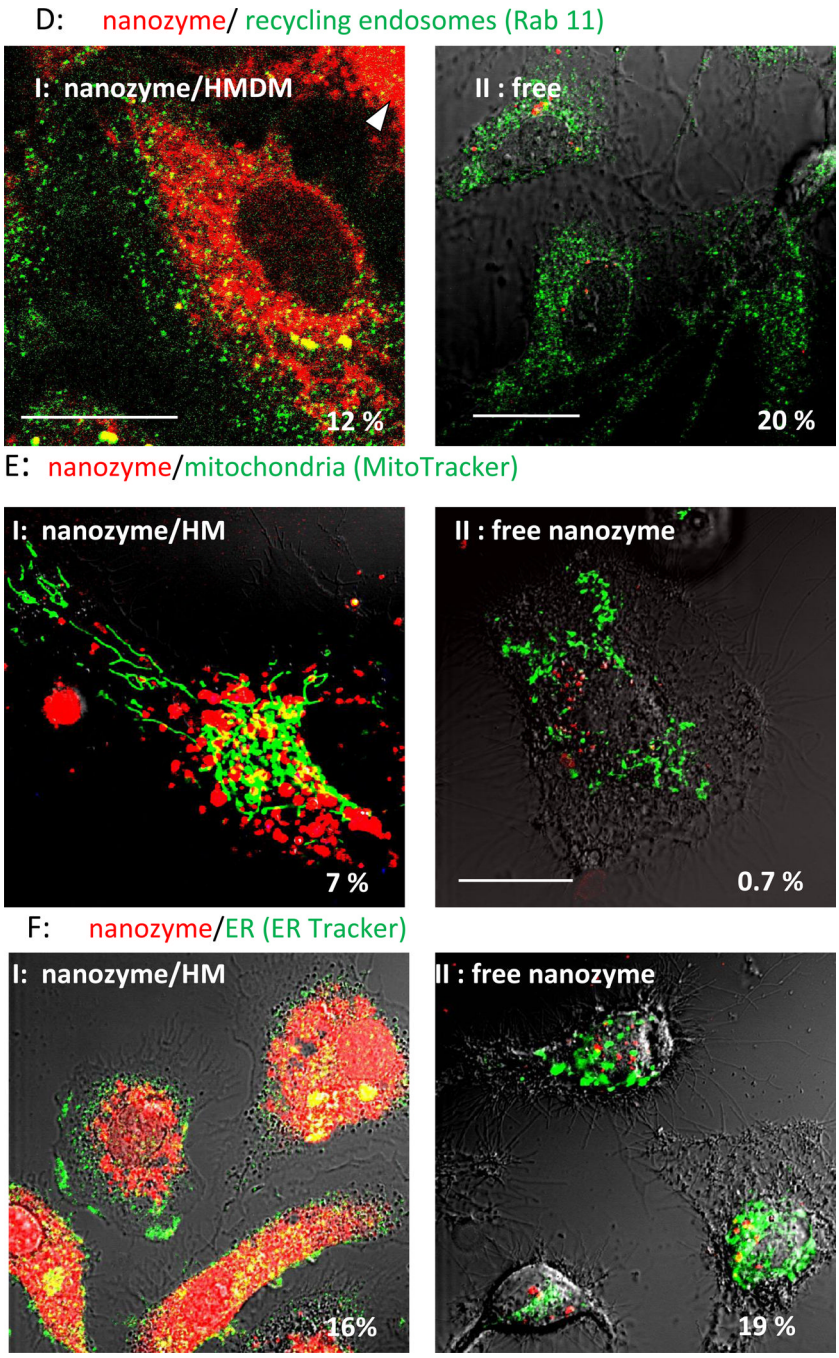

Figure 8. Intracellular localization of cell-derived or cell-free nanozyme within HBMEC

HBMEC were incubated for 30 min with (**I**) human macrophages preloaded with nanozyme, or (**II**) cell-free nanozyme (without carrier cells), fixed, permeabilized, and stained with (**A**) FITC-conjugated EEA1 monoclonal antibody (to early endosomes); (**B**) mouse monoclonal antibody Rab7 (late endosomes); (**C**) FITC-conjugated LAMP 1 monoclonal Ab (to lysosomes); (**D**) mouse monoclonal antibody to Rab11 (recycling endosomes); (**E**) Mitotracker Green; (**F**) ER Tracker Green. Cells labeled with unconjugated primary mouse antibody (**B, C**) were stained with FITC-conjugated secondary goat anti-mouse immunoglobulin G. To distinguish between carrier cells and target cells, human

macrophages were labeled with Alexa Fluor-405-conjugated anti-CD14 (blue) (**A, E**). Colocalization of nanozyme (red) and compartment staining (green) was manifested in yellow. Human macrophages are shown by arrowheads. Refer also to Table 2 for quantitative colocalization. Bar = 20 μm.

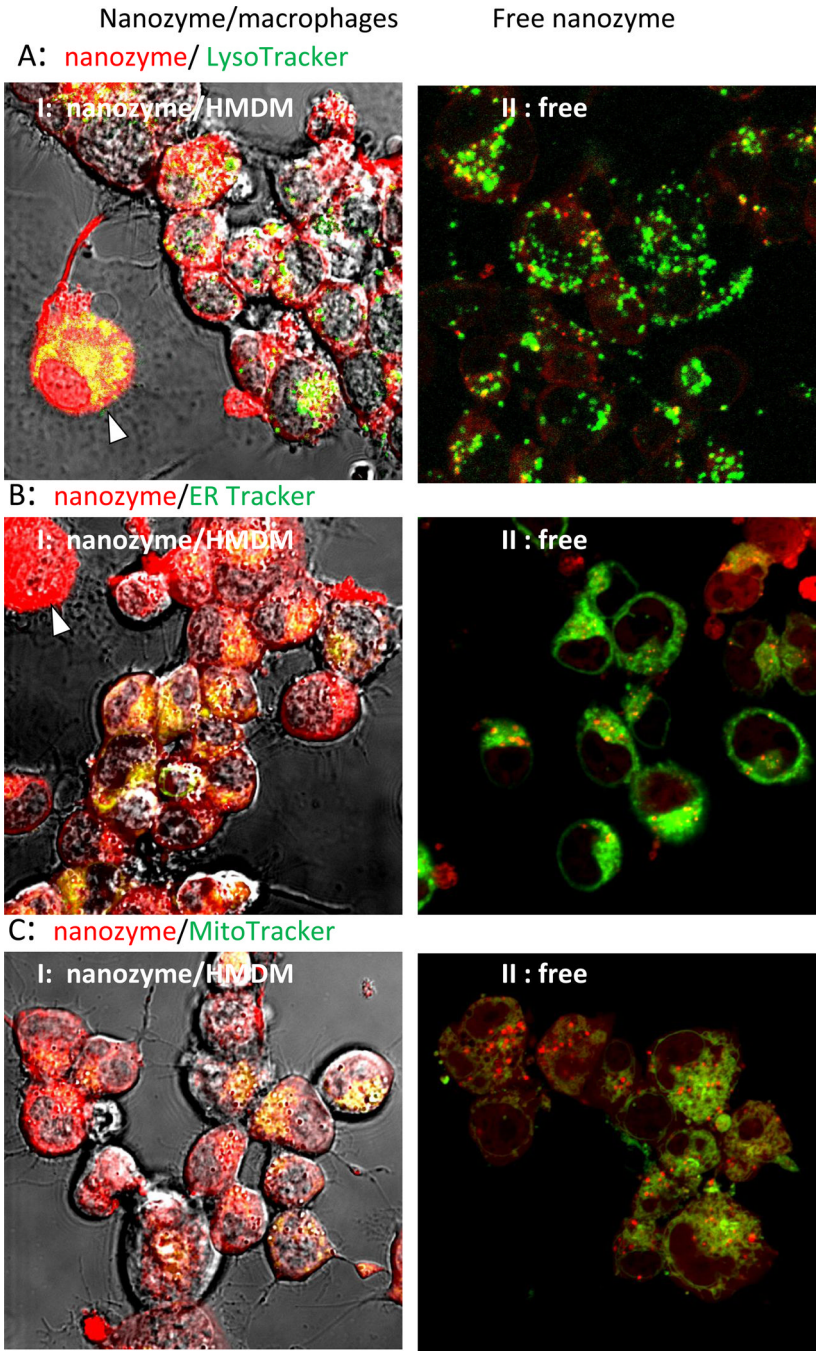

Figure 9. Intracellular localization of cell-derived or cell-free nanozyme within CATH.a neurons

CATH.a neurons were incubated for 18 hours with (**I**) murine macrophages preloaded with nanozyme, or (**II**) cell-free nanozyme (without carrier cells), washed and stained with (**A**) Mitotracker green; (**B**) ER tracker Green; or (**C**) Lysotracker green. Colocalization of nanozyme (red) and compartment staining (green) is shown in yellow. Murine macrophages are shown by arrowheads. Refer also to Table 2 for quantative colocalization. Bar = 20 μm.

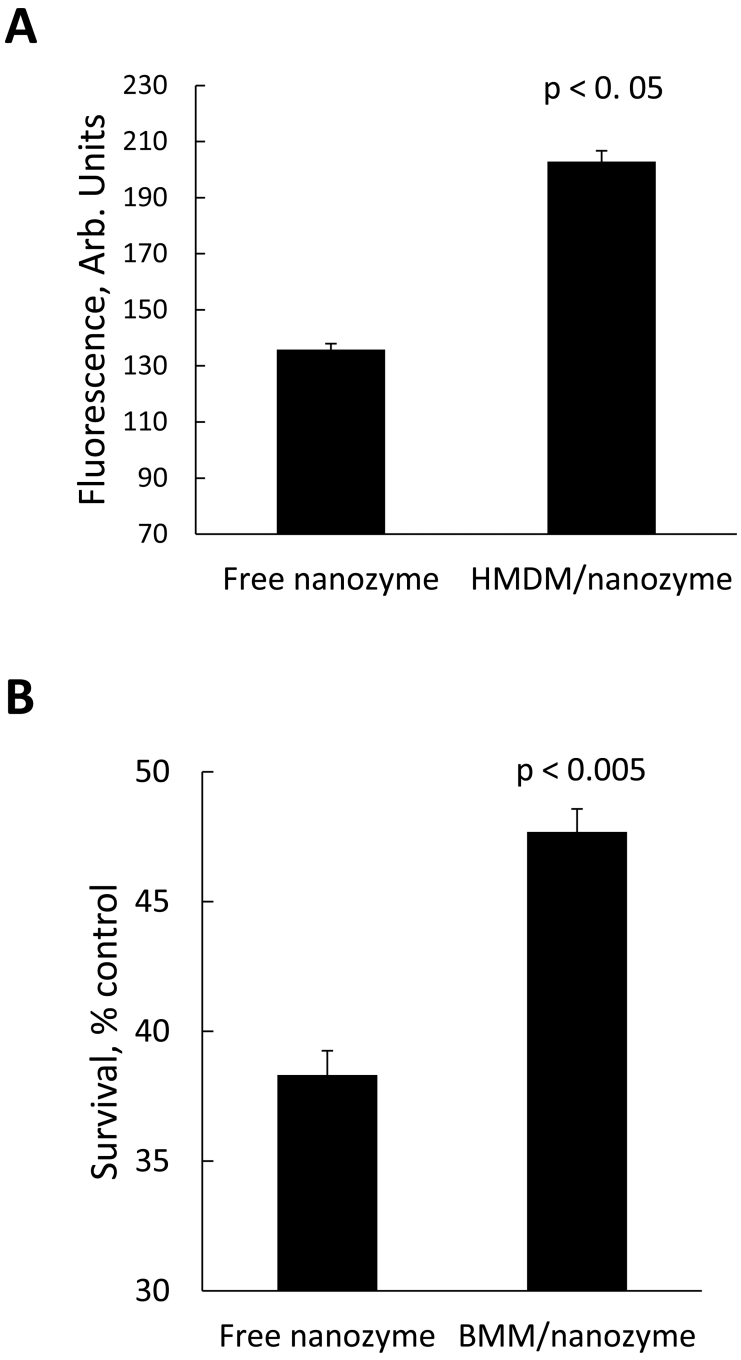

Figure 10. Superior transport and neuroprotective activity of nanozyme loaded in macrophages compared to cell-free nanozyme

(**A**) Effect of nanozyme loading into human macrophages on its accumulation in HBMEC: the recipient cells were incubated with cell free nanozyme or exposed to macrophages loaded with fluorescently-labeled nanozyme for four hours. Following incubation, the cells were collected and the amount of nanozyme accumulated in HBMEC was determined by FACS. (**B**) Effect of nanozyme loading into murine macrophages on its neuroprotective activity in *in vitro* PD model: CATH.A neurons were incubated with 6-OHDA in the presence of murine macrophages loaded with nanozyme or the same amount of free nanozyme for four hours. Following incubation, the cells were washed, stained with LIVE/

DEAD dye and neuronal survival accessed by FACS. Data are expressed as % of control cells cultured in the media. To distinguish between the carrier cells and target cells, human and murine macrophages were labeled with Alexa 678-conjugated Ab to CD 14 and CD 11b, respectively, prior to the addition. Results from N=4 wells (± SEM) clearly demonstrated that transport to HBMEC (**A**), and neuroprotective activity (**B**) of nanozyme from the cell-carriers, were substantially greater, compared to the transport and activity of free nanozyme.

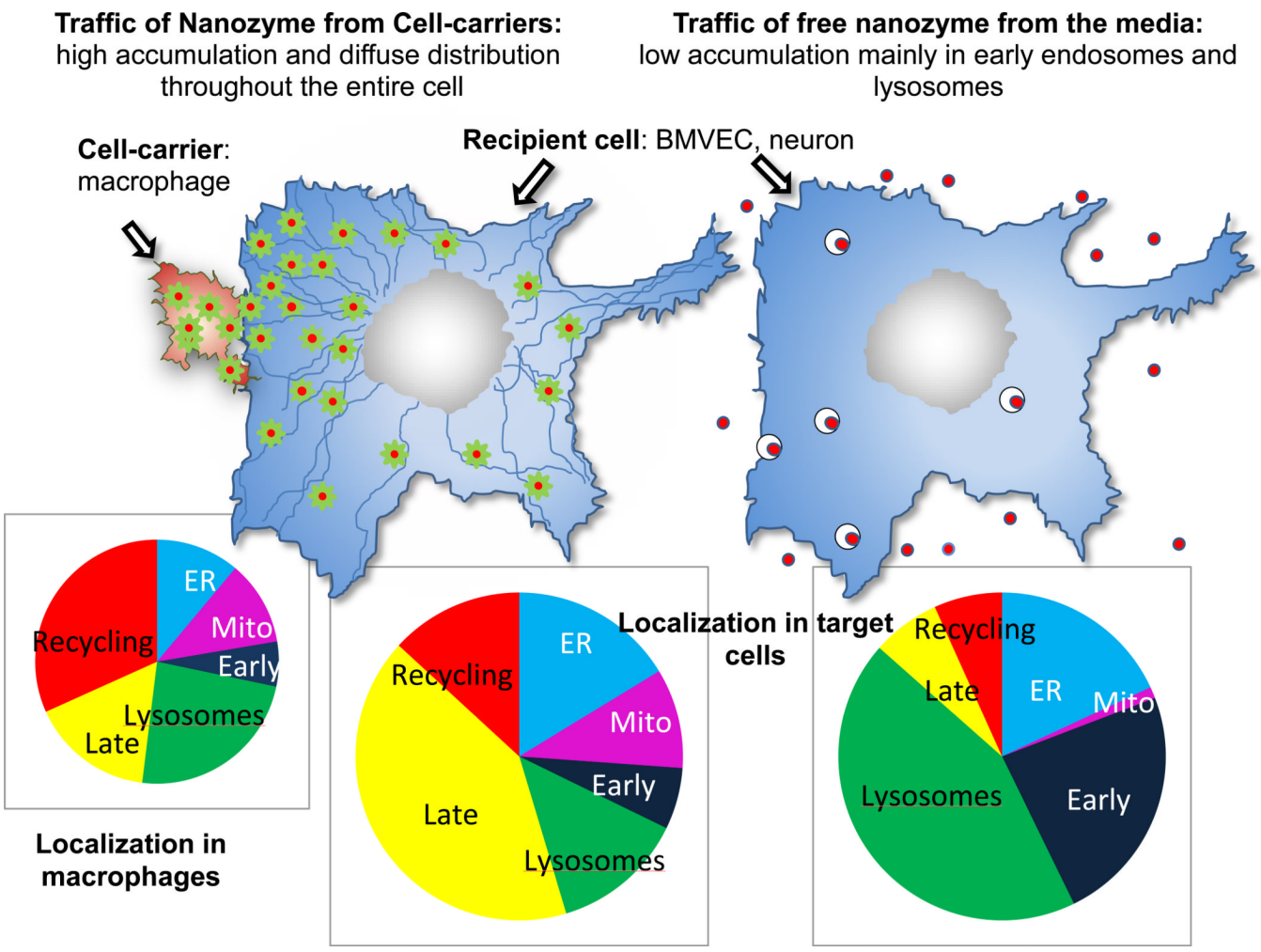

Figure 11. Nanozyme intracellular localization in recipient cells transferred from carrier cells or from media

Encapsulation of nanozyme into exosomes from the carrier cells allowed their efficient fusion with the plasma membranes of target cells, and favorable intracellular localization in contrast to free nanozyme taken from the media and accumulated in endosomal compartments. Exosomes with incorporated nanozyme travel in target cells using them like tracks.

Table 1

Evaluation of Nanozyme Entrance, Intracellular Trafficking, and Release by % Colocalization with Specific Intracellular Compartments in Carrier Cells, Human Macrophages

Organelle	5 min	15 min	30 min	60 min
Entrance				
clatrin-coated pits	35.1 ± 2.2[b]	29.0 ± 1.1	21.6 ± 3.4	43.0 ± 3.9
caveolae	4.9 ± 1.9	2.2 ± 1.2	2.9 ± 0.2	1.3 ± 0.2
Intracellular trafficking				
Acidic organelles	49.5 ± 6.2	56.6 ± 4.1	58.4 ± 3.4	61.0 ± 3.9
ER	18.3 ± 5.0	10.2 ± 4.9	14.6 ± 1.4	16.8 ± 1.5
Mitochondria	12.5 ± 1.6	9.7 ± 1.0	18.5 ± 2.3	17.0 ± 2.0
Early endosomes	13.0 ± 4.9	4.68 ± 2.2	7.2 ± 1.4	9.0 ± 0.8
Late endosomes	13.4 ± 1.5	9.9 ± 1.7	30.0 ± 3.8	24.7 ± 3.2
Recycling endosomes	35.0 ± 1.5	26.1 ± 2.2	26.2 ± 2.1	47.4 ± 9.5
Lysosomes	23.4 ± 6.7	11.13 ± 1.9	19.6 ± 3.8	35.8 ± 4.9
Release [a]				
	non-activated		activated with LPS and IFN-γ	
Actin microfilaments	26.1 ± 0.1		79.1 ± 7.2	

[a] nanozyme-preloaded murine macrophages were incubated with CATH.A neurons for 18 hours

[b] Data represent means ± SEM (N = 40).

Table 2

Evaluation of Nanozyme Entrance and Intracellular Trafficking by % Colocalization with Specific Intracellular Compartments in in Target Cells, HBMEC

Organelle	from macrophages[a]		free, from media	
	30 min	60 min	30 min	60 min
Entrance				
actin	13.1 ± 2.5 [b]	19.0 ± 1.4	n/a	n/a
tubulin	58.0 ± 4.3	44.5 ± 2.5	n/a	n/a
Intracellular trafficking				
ER	9.6 ± 21.7	16.3 ± 1.0	18.7 ± 1.9	19.1 ± 1.0
Mitochondria	8.9 ± 1.1	6.9 ± 0.7	1.1 ± 0.3	0.7 ± 1.4
Early endosomes	4.2 ± 0.9 (*)	17.2 ± 1.6 (*)	15.2 ± 3.3	26.9 ± 1.7
Late endosomes	29.5 ± 1.4 (**)	22.4 ± 1.3 (**)	4.3 ± 0.7	12.2 ± 2.1
Recycling endosomes	9.5 ± 1.4 (*)	11.8 ± 1.1 (*)	4.4 ± 0.4	19.7 ± 2.1
Lysosomes	9.6 ± 2.4 (*)	11.0 ± 2.0 (*)	27.8 ± 4.4	19.4 ± 2.4

[a] Statistical significance compared to colocalization levels of macrophages-free nanozyme accumulated from the media is shown by asterisk: $p<0.05$ (*); $p<0.005$ (**).

[b] Data represent means ± SEM (N = 40).